GEOLOGY | THE GEOLOGICAL SOCIETY OF AMERICA®

https://doi.org/10.1130/G51318.1

Manuscript received 26 July 2022
Revised manuscript received 19 April 2023
Manuscript accepted 20 July 2023

Published online 2 August 2023

© 2023 The Authors. Gold Open Access: This paper is published under the terms of the CC-BY license.

Magma mingling and ascent in the minutes to hours before an explosive eruption as recorded by banded pumice

Hannah I. Shamloo[1,*] and Anita L. Grunder[2]
[1]Department of Geological Sciences, Central Washington University, Ellensburg, Washington 98926, USA
[2]College of Earth, Ocean, and Atmospheric Sciences, Oregon State University, Corvallis, Oregon 97331, USA

ABSTRACT

High-threat explosive silicic eruptions commonly contain banded pumice, reflecting magma mingling in the conduit prior to or during eruption. Heterogeneities in tuffs have been attributed to the draw-up of compositionally distinct magmas, in which low-viscosity magmas ascend more quickly than high-viscosity magmas. The Rattlesnake Tuff of the High Lava Plains in Oregon (northwestern United States) represents a zoned magma reservoir where at least five different rhyolite compositions are preserved in banded pumice samples in variable mingled combinations. Geochemical gradients recorded across band boundaries in pumice were modeled using a Monte Carlo least-square minimization procedure to find the complementary error function that best fit observed Si and Ba diffusion profiles by iteratively varying the concentration of each plateau (i.e., the concentration on either side of the band boundary), the center and spacing of the diffusion profile, diffusion length scale, and temperature. Modeling indicates maximum time scales between mingling and conduit ascent from minutes to hours. Viscosity calculations for each rhyolite composition confirm that highly viscous rhyolites have longer ascent times than low-viscosity magmas, strongly supporting a model of sequential tapping of a zoned chamber controlled by viscosity.

HETEROGENEITIES IN TEPHRA

Explosive silicic eruptions produce pyroclastic density currents that can cover landscapes and threaten human populations and agriculture, and even affect global climate. Despite the risk associated with these events, questions remain regarding the pre-eruptive configuration of magma as well as the timing of magma ascent and eruption. Many explosive deposits contain heterogeneities as (1) chemically or thermally zoned ignimbrites indicating heterogeneities in the pre-eruptive magma configuration itself, and/or (2) the presence of banded pumice indicating the simultaneous tapping of distinct compositions upon eruption (e.g., Lipman, 1967; Hildreth, 1979, 1981; Spera et al., 1986; Grunder and Mahood, 1988; Bacon and Druitt, 1988; Wolff et al., 1990; Hildreth and Fierstein, 2000; Aguirre-Díaz, 2001; Bacon and Lanphere, 2006; Pabst et al., 2008; Huber et al., 2012; Ellis et al., 2014; Bachmann and Huber, 2016). Moreso, the compositional layering (i.e., bands) in banded pumice (which are commonly intricately layered and folded) indicates the fluid mingling of distinct magma types during magma ascent in the conduit itself (e.g., Andrews and Manga, 2014). Furthermore, the preservation of such sharp bands implies that the duration of time for distinct magmas to be juxtaposed was short.

Through mathematical analysis, Blake (1981) attributed zoning in ignimbrites and compositionally banded pumice to the evacuation of magma by a series of successive spherical sampling shells that increase in volume with time and intersect with density-stratified horizontal layers in a magma chamber (Fig. 1A). This way, less-viscous magma draws up more quickly, leading to mingling of distinct magmas in the conduit upon and during ascent and eruption (Blake and Ivey, 1986; Spera et al., 1986). What has yet to be done is to confirm this model (Fig. 1A) by quantitatively determining the time scales of magma mingling and their subsequent ascent, which is important for interpreting petrologic and seismic evidence of magma recharge and eruption triggering (e.g., Eichelberger, 1980; Ruprecht et al., 2008; Wright et al., 2011; Till et al., 2015; Shamloo and Till, 2019; Bardelli et al., 2020; Shamloo et al., 2021).

Diffusion chronometry is a powerful tool for estimating time scales using the chemical gradients recorded in zoned erupted material but is commonly applied to mineral zoning (e.g., Costa et al., 2020, and references therein). Glass zoning (i.e., the contact between distinct bands in pumice), on the other hand, has been underutilized by diffusion chronometry, despite also experiencing elemental diffusion across zone boundaries, which is recorded as chemical gradients rather than an abrupt step in composition. In the case of banded pumice, we assume the chemical gradient represents the timing between the first contact between two rhyolite compositions in the conduit (i.e., magma mingling) and their eruption, when diffusion ceases. Here, we apply diffusion chronometry to the chemical gradients recorded across the boundaries within banded pumice to estimate the timing of magma mingling and ascent. In addition, we test the role of viscosity as proposed by Blake (1981) where less-viscous materials ascend faster than more-viscous materials and lead to heterogeneities in explosive eruptive products. The novel technique of applying diffusion chronometry to vesiculated material poses many additional challenges. Our method serves as a proof of concept, demonstrating the ability to calculate time scales of pre- and syn-eruptive magmatic processes associated with threatening explosive eruptions using a commonly observed rock type.

BANDED PUMICE OF THE RATTLESNAKE TUFF, HIGH LAVA PLAINS, EASTERN OREGON

Spectacular dark-light banding preserved in pumices of the Rattlesnake Tuff make it the target of this study (Fig. 2; Fig. S1 in the Supplemental Material[1]). The ca. 7 Ma Rattlesnake

Hannah Shamloo https://orcid.org/0000-0003-2500-2988
*shamlooh@cwu.edu

[1]Supplemental Material. Additional figures with discussion of analytical and modeling methods (File S1: Figs. S1–S6), data collected (File S2: Tables S1–S4), and Python script (File S3). Please visit https://doi.org/10.1130/GEOL.S.23749350 to access the supplemental material, and contact editing@geosociety.org with any questions.

CITATION: Shamloo, H., and Grunder, A., 2023, Magma mingling and ascent in the minutes to hours before an explosive eruption as recorded by banded pumice: Geology, v. 51, p. 957–961, https://doi.org/10.1130/G51318.1

Downloaded from http://pubs.geoscienceworld.org/gsa/geology/article-pdf/51/10/957/5951746/g51318.1.pdf
by guest

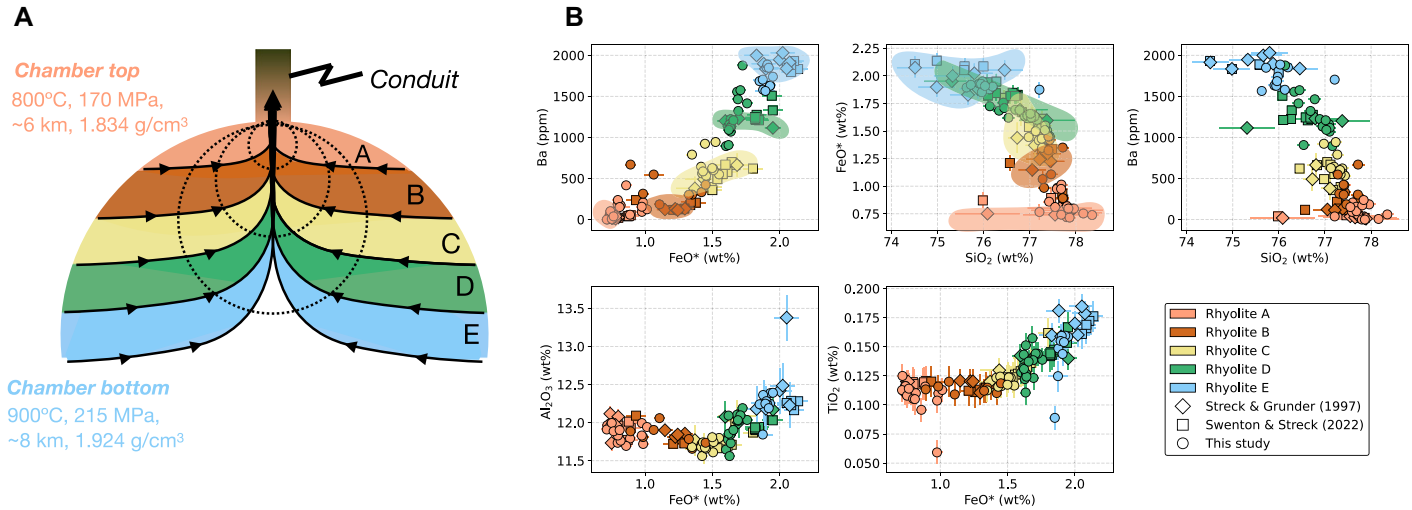

Figure 1. (A) Schematic representation of the pre-eruptive configuration of the Rattlesnake Tuff magma reservoir based on compositional variability of banded pumice (Streck and Grunder 1995, 1997; Swenton and Streck, 2022). Rhyolite groups A through E refer to distinct compositional types based on groupings shown in B. Dashed circles represent spherical shells successively sampled upon eruption, after Blake (1981). Black arrows represent flow paths of magma draw-up between compositional boundaries. Temperature, pressure, depth, and density estimates are provided for inferred top and bottom of the chamber (Streck and Grunder, 1997; Swenton and Streck, 2022). (B) Element variation diagrams collected via electron microprobe of distinct rhyolite groups preserved within Rattlesnake Tuff banded pumice. FeO* represents total Fe, and the error bars represent the uncertainty in concentration measurements via electron microprobe. Streck and Grunder (1997) data are shown by diamonds and outlined by shaded regions in the first two panels. Data are colored coded (or compositionally binned) based on the respective rhyolite group after the characterization established by Streck and Grunder (1997) and Swenton and Streck (2022).

Tuff eruption is part of basalt-rhyolite volcanism in the High Lava Plains of eastern Oregon (northwestern United States) (Fig. S2; Streck and Grunder, 1995, 1997, 2008; Laib, 2016) resulting in a poorly welded to nonwelded tuff with an estimated magmatic volume of 280 km³. Rhyolites within this single eruptive unit fall into five compositionally distinct rhyolite groups (A–E; Fig. 1B; Fig. S3), characterized mainly by variations in Si, Ba, and Fe but also minor and trace elements including Ti, La, Eu, Ta, Nb, Zr, Hf, Rb, Cs, Th, and U (Fig. S3; Streck and Grunder, 1997; Swenton and Streck, 2022). As many as four groups have been documented in a single sample (Swenton and Streck, 2022). Pumice are finely vesicular throughout (typically ~70% vesicularity), with vesicle sizes ranging from a few microns to >100 μm wide (Fig. S4).

Swenton and Streck (2022) verified that the five distinct rhyolite types (A–E) were likely stratified by density (Streck and Grunder, 1997) and experienced little to no chemical mixing prior to eruption. Their density calculations show that the less-dense rhyolite A, with the most evolved composition, resided at the top of the magma reservoir and rhyolite E at the bottom (Fig. 1A; Streck and Grunder, 1997; Swenton and Streck, 2022). This interpretation is supported by rhyolite A occurring alone at the base of the eruptive unit, indicating it was the first composition to erupt (Streck and Grunder, 1997). The boundaries between bands in rhyolite pumice are sharp to crenulate, suggesting they were not in contact for very long, and mechanical mixing (or mingling) likely occurred within the conduit itself upon and during ascent.

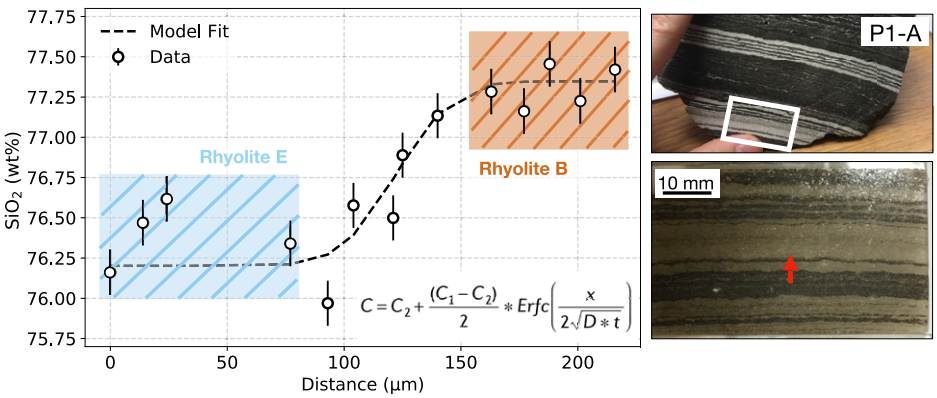

Figure 2. Electron microprobe transect measured across a band boundary in Rattlesnake Tuff pumice. Best-fit solution to the diffusion equation is shown by the dashed line (for modeling details, see text). The diffusion equation is included in the lower right corner, where *C* is the normalized concentration, C_1 and C_2 are the initial amounts of the elements on each side of the interface at time zero, D_i is the calculated diffusivity in m²/s, *t* is the diffusion time, and *x* is the midpoint of concentration gradient. Location of probe transect (red arrow) is shown on photo of thin section in bottom right, and associated hand sample is shown in upper right. Shaded boxes are shown to demonstrate how plateau data points on each side of the profile were averaged and used to characterize into a respective rhyolite group. Here, the profile represents timing between mingling and eruption for rhyolite E with B.

In addition to being density stratified, the pre-eruptive Rattlesnake Tuff magma was thermally zoned (Fig. 1A). Rhyolite E storage temperature was 900 ± 70 °C and rhyolite A was 800 ± 40 °C (rhyolite-MELTS thermometry; Swenton and Streck, 2022). Quartz-albite-orthoclase and clinopyroxene barometry yield pressures between 170 (rhyolites A and B) and 215 MPa (rhyolites C, D, and E), or ~6–8 km depth (Swenton and Streck, 2022). Rhyolite A was likely water saturated, whereas the other rhyolites were barely undersaturated, as inferred from the position of rhyolite compositions relative to the water-saturated minimum in haplogranite ternary space (Streck and Grunder, 1997).

ELEMENTAL DIFFUSION ACROSS PUMICE BAND BOUNDARIES

Chemical gradients of major and minor elements were measured across band boundaries using an electron microprobe with variable spac-

Downloaded from http://pubs.geoscienceworld.org/gsa/geology/article-pdf/51/10/957/5951746/g51318.1.pdf
by guest

ing depending on the available pumice surface (Fig. 2; Table S1 and Fig. S5 in the Supplemental Material). Note that not all measured transects yielded resolvable diffusion profiles but all are included in Table S1. The data in the distal plateaus (i.e., the elemental concentrations on each side of the band boundary) were averaged and assigned a rhyolite composition based on the criteria from previous studies to establish mingled end members and therefore spatial context for the mingling and ascent time calculated (Fig. 1B; Streck and Grunder, 1997; Swenton and Streck, 2022). A full suite of trace elements was not analyzed, and therefore not all the discriminants of previous work are applied.

Diffusion modeling was employed using Si and/or Ba zoning (preferably both where both elemental profiles were resolvable on the probe) across the boundaries between distinct bands within Rattlesnake Tuff pumice samples (Fig. 2). The measured concentration profiles were modeled with a Monte Carlo least-square minimization procedure implemented in Python to find the complementary error function that best fit each observed element profile assuming an initial condition of a step function that physically represents the first contact of mechanical mingling between rhyolites (Fig. 2; Fig. S5). Arrhenius parameters for Ba were used from Magaritz and Hofmann (1978), which were determined for high-silica rhyolites with conditions relevant to the Rattlesnake Tuff (Table S3). Arrhenius parameters for Si were less straightforward, and instead two diffusivities for Si in rhyolite (i.e., Si in rhyolite with 3 versus 6 wt% H_2O; Baker, 1991) were tested. Water content for the Rattlesnake Tuff has been placed at 2–4 wt% H_2O and no more than 5 wt% H_2O based on rhyolite-MELTS modeling (Swenton and Streck, 2022). The exact water content in the conduit between mingled pairs is unknown, but when modeling Si profiles using the diffusivity of Si in rhyolite with 6 wt% H_2O, the resulting time scales disagree with Ba time scales. In addition, the general width of the Ba and Si profiles are the same, indicating that they record similar amounts of diffusive relaxation; therefore, we favor the time results using diffusivity of Si in rhyolite with 3 wt% H_2O, which yield time scales that agree with Ba time scales.

To best account for sources of error introduced from performing diffusion chronometry on vesiculated material, the model iteratively varied the concentration of each plateau by creating a Monte Carlo synthetic normal distribution of possible plateau values (after Brugman et al., 2022) as well as varying the center of the diffusion profile to account for the uncertainty in distance and the uneven spacing of measurements to avoid vesicles during measurement. A range of temperatures was modeled based on thermometry results for each Rattlesnake Tuff rhyolite group (e.g., 760–970 °C; File S1). The diffusion length scale (i.e., the square root of the product of the diffusion coefficient and time) was varied by calculating a range of diffusion coefficients using the uncertainties in Arrhenius parameters D_0 and E_A (pre-exponential factor and activation energy). Therefore, rather than reporting a "best-fit time," the model reported results as a best-fit profile that produced the lowest misfit between measured and modeled gradients from a combination of time–temperature–diffusion coefficient values (Brugman et al., 2022). A cumulative distribution function of times was produced for a given profile, where the 5th and 95th percentile of the distribution was taken as the reported minimum and maximum values in a given time interval (Fig. 3; Table S2).

Lastly, while our modeling approach tries to account for uncertainty in the measured profile itself, we acknowledge the additional limitations to this study (further discussed in File S1). For example, if vesiculation were to have occurred during or after diffusion, then the diffusion length would have been expanded, yielding an apparently longer diffusion time. This is a likely scenario given that the Rattlesnake Tuff magma was stored at relatively shallow pressures and was water saturated. This implies that calculated time scales here represent maxima. Additionally, a sensitivity test was performed by fitting multiple profiles from the same boundary but with variable degrees of vesicularity (File S2). We find time scales within error of each other (e.g., combination CD in Fig. 3), which indicates either fine differences in time scales are lost in the spatial resolution of our measurements, or the differences in time scales are enveloped in the error associated with best-fit time intervals.

THE TIMING OF MINGLING AND ERUPTION OF RATTLESNAKE TUFF RHYOLITES

In general, diffusion times range from minutes to hours depending on the rhyolite members involved in mingling. The most striking observation is that time scales involving the mingling of rhyolite A (i.e., combinations AE and AD in Fig. 3) are generally longer than time scales involving the mingling of rhyolite B and C (i.e., BE and CD in Fig. 3). For example, the average time scale for mingled rhyolites A and E is 630^{+430}_{-160} min or 10^{+7}_{-3} hr, whereas the average time scale for mingled rhyolites C and D is an order of magnitude shorter at 8^{+6}_{-1} min.

Based on its proximity to the conduit, rhyolite A should theoretically have been the first magma to enter the conduit and erupt, which is reflected in the field observations of rhyolite A being at the base of most sections (Streck and Grunder, 1997). Therefore, it is possible that rhyolite A generally spent the most time in the conduit, contributing to the longer time scales observed from our data set.

Another factor that could have led to longer time scales for mingled pairs involving rhyolite A is viscosity—where low-viscosity magmas are drawn up more quickly than high-viscosity magmas as originally proposed by Blake (1981).

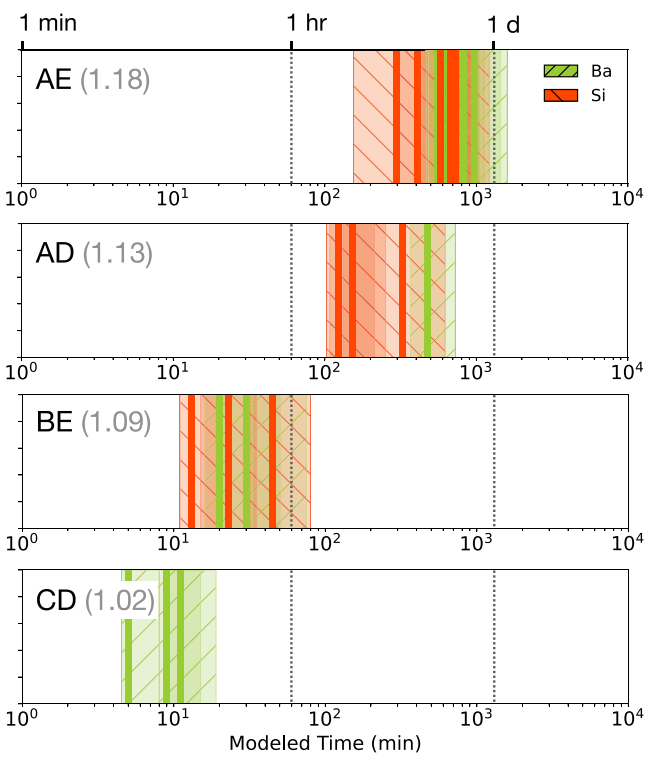

Figure 3. Summary of calculated diffusion times for both Si and Ba. Diffusion times are presented in separate panels by their respective rhyolite mingling combinations. The two-letter identifier in each panel indicates the two rhyolite groups involved in mingling (see Fig. 1 for explanation of the five groups). Thick vertical lines are best-fit time, and shaded region surrounding each best-fit time is the associated error envelope. Viscosity contrast ratios are reported in parentheses and calculated by dividing the average viscosity of the higher-viscosity magma by the average viscosity of the lower-viscosity magma.

Downloaded from http://pubs.geoscienceworld.org/gsa/geology/article-pdf/51/10/957/5951746/g51318.1.pdf
by guest

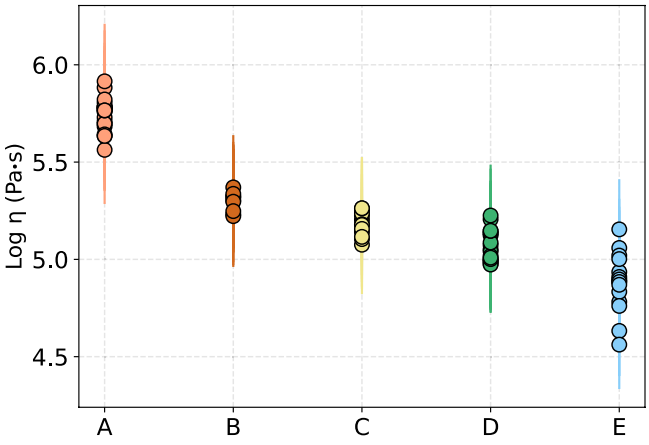

Figure 4. Viscosities (η) calculated for Rattlesnake Tuff pumice samples representing five distinct rhyolite compositions (A–E; see Fig. 1). Error bars represent the uncertainty in viscosity calculations. Calculations were performed after Giordano et al. (2008), assuming variable temperature and volatile contents for each respective rhyolite.

Viscosity calculations were performed for each distinct rhyolite composition preserved in the banded pumice (Fig. 4; Table S4). As expected, rhyolite A is the most viscous relative to the other rhyolites (i.e., rhyolite A: $10^{5.6–5.8}$ Pa·s; rhyolite E: $10^{4.6–5.2}$ Pa·s) based on its chemical composition, water content, inferred temperature, and crystal content (<1 vol%; Streck and Grunder, 1997; Swenton and Streck, 2022) likely contributing to the longer time scales associated with the mingling and ascent of rhyolite A. Additionally, viscosity contrast ratios were calculated for each mingled pair, illustrating that the higher the viscosity contrast, the longer the ascent times. These results potentially provide predictive power to ascent times of magmas based on their viscosities.

Conduit ascent rates are calculated assuming the shallowest pressure recorded by Rattlesnake Tuff pumice marks the roof of the chamber and therefore the base of the conduit (i.e., 170 MPa ≈ 6 km; Swenton and Streck, 2022). Generally, ascent rates range from 10^1 to 10^3 m/s (Table S3). These are in broad agreement with ascent rates determined from other explosive eruptions using other diffusion techniques (e.g., Fig. S6; Humphreys et al., 2008; Myers et al., 2016; Newcombe et al., 2020).

CONCLUDING REMARKS

We conclude maximum conduit ascent times for an explosive rhyolite eruption are on the order of minutes to hours and are strongly controlled by magma viscosity. While many limitations exist within this approach, this study serves as a proof of concept that diffusion chronometry across compositional boundaries in banded pumice can be used to calculate pre- and syn-eruptive time scales for threatening volcanic eruptions. This work also provides support to numerical models related to magma flow conduits.

ACKNOWLEDGMENTS

The authors thank Vanessa Swenton and Martin Streck for sharing Rattlesnake Tuff samples, Marie Takach for assistance with the electron microprobe, Kevin Pendergast for foundational undergraduate work, Kara Brugman for coding expertise and advice, and Scott Boroughs for collecting additional probe images and data. Thank you to Joseph Boro, Jamshid Moshrefzadeh, and an anonymous reviewer who provided constructive feedback that greatly improved this manuscript. This work was supported by a National Science Foundation (NSF) EAR Postdoctoral Fellowship (1952808) awarded to Shamloo and an NSF grant awarded to Grunder (1939347).

REFERENCES CITED

Aguirre-Díaz, G.J., 2001, Recurrent magma mingling in successive ignimbrites from Amealco caldera, central Mexico: Bulletin of Volcanology, v. 63, p. 238–251, https://doi.org/10.1007/s004450100138.

Andrews, B.J., and Manga, M., 2014, Thermal and rheological controls on the formation of mafic enclaves or banded pumice: Contributions to Mineralogy and Petrology, v. 167, 961, https://doi.org/10.1007/s00410-013-0961-7.

Bachmann, O., and Huber, C., 2016, Silicic magma reservoirs in the Earth's crust: American Mineralogist, v. 101, p. 2377–2404, https://doi.org/10.2138/am-2016-5675.

Bacon, C.R., and Druitt, T.H., 1988, Compositional evolution of the zoned calcalkaline magma chamber of Mount Mazama, Crater Lake, Oregon: Contributions to Mineralogy and Petrology, v. 98, p. 224–256, https://doi.org/10.1007/BF00402114.

Bacon, C.R., and Lanphere, M.A., 2006, Eruptive history and geochronology of Mount Mazama and the Crater Lake region, Oregon: Geological Society of America Bulletin, v. 118, p. 1331–1359, https://doi.org/10.1130/B25906.1.

Baker, D.R., 1991, Interdiffusion of hydrous dacitic and rhyolitic melts and the efficacy of rhyolite contamination of dacitic enclaves: Contributions to Mineralogy and Petrology, v. 106, no. 4, p. 462–473, https://doi.org/10.1007/BF00321988.

Bardelli, L., Arnosio, M., Báez, W., Suzaño, N., Becchio, R., Viramonte, J., Bustos, E., and Bertea, E., 2020, Multi-banded pumice in the Campo de la Piedra Pómez rhyolitic ignimbrite (Southern Puna plateau): Pre-eruptive physical and chemical interactions between mafic and rhyolitic melts: Journal of South American Earth Sciences, v. 101, https://doi.org/10.1016/j.jsames.2020.102616.

Blake, S., 1981, Volcanism and the dynamics of open magma chambers: Nature, v. 289, p. 783–785, https://doi.org/10.1038/289783a0.

Blake, S., and Ivey, G.N., 1986, Magma-mixing and the dynamics of withdrawal from stratified reservoirs: Journal of Volcanology and Geothermal Research, v. 27, p. 153–178, https://doi.org/10.1016/0377-0273(86)90084-3.

Brugman, K., Till, C.B., and Bose, M., 2022, Common assumptions and methods yield overestimated diffusive timescales, as exemplified in a Yellowstone post-caldera lava: Contributions to Mineralogy and Petrology, v. 177, 63, https://doi.org/10.1007/s00410-022-01926-5.

Costa, F., Shea, T., and Ubide, T., 2020, Diffusion chronometry and the timescales of magmatic processes: Nature Reviews Earth & Environment, v. 1, p. 201–214, https://doi.org/10.1038/s43017-020-0038-x.

Eichelberger, J.C., 1980, Vesiculation of mafic magma during replenishment of silicic magma reservoirs: Nature, v. 288, p. 446–450, https://doi.org/10.1038/288446a0.

Ellis, B.S., Bachmann, O., and Wolff, J.A., 2014, Cumulate fragments in silicic ignimbrites: The case of the Snake River Plain: Geology, v. 42, p. 431–434, https://doi.org/10.1130/G35399.1.

Giordano, D., Russell, J.K., and Dingwell, D.B., 2008, Viscosity of magmatic liquids: A model: Earth and Planetary Science Letters, v. 271, p. 123–134, https://doi.org/10.1016/j.epsl.2008.03.038.

Grunder, A.L., and Mahood, G.A., 1988, Physical and chemical models of zoned silicic magmas: The Loma Seca Tuff and Calabozos caldera, southern Andes: Journal of Petrology, v. 29, p. 831–867, https://doi.org/10.1093/petrology/29.4.831.

Hildreth, W., 1979, The Bishop Tuff: Evidence for the origin of compositional zonation in silicic magma chambers, *in* Chapin, C.E., and Elston, W.E., eds., Ash-Flow Tuffs: Geological Society of America Special Paper 180, p. 43–76, https://doi.org/10.1130/SPE180-p43.

Hildreth, W., 1981, Gradients in silicic magma chambers: Implications for lithospheric magmatism: Journal of Geophysical Research, v. 86, p. 10,153–10,192, https://doi.org/10.1029/JB086iB11p10153.

Hildreth, W., and Fierstein, J., 2000, Katmai volcanic cluster and the great eruption of 1912: Geological Society of America Bulletin, v. 112, p. 1594–1620, https://doi.org/10.1130/0016-7606(2000)112<1594:KVCATG>2.0.CO;2.

Huber, C., Bachmann, O., Vigneresse, J.-L., Dufek, J., and Parmigiani, A., 2012, A physical model for metal extraction and transport in shallow magmatic systems: Geochemistry, Geophysics, Geosystems, v. 13, Q08003, https://doi.org/10.1029/2012GC004042.

Humphreys, M.C., Menand, T., Blundy, J.D., and Klimm, K., 2008, Magma ascent rates in explosive eruptions: Constraints from H_2O diffusion in melt inclusions: Earth and Planetary Science Letters, v. 270, no. 1–2, p. 25–40, https://doi.org/10.1016/j.epsl.2008.02.041.

Laib, A.C., 2016, Pre-eruptive timescales and processes of large shallow magma systems revealed by compositional variability in silicic ignimbrites [Ph.D. thesis]: Boise, Idaho, Boise State University, 186 p.

Lipman, P.W., 1967, Mineral and chemical variations within an ash-flow sheet from Aso caldera, southwestern Japan: Contributions to Mineralogy and Petrology, v. 16, p. 300–327, https://doi.org/10.1007/BF00371528.

Magaritz, M., and Hofmann, A.W., 1978, Diffusion of Sr, Ba and Na in obsidian: Geochimica et Cosmochimica Acta, v. 42, no. 6, p. 595–605, https://doi.org/10.1016/0016-7037(78)90004-2.

Myers, M.L., Wallace, P.J., Wilson, C.J., Morter, B.K., and Swallow, E.J., 2016, Prolonged ascent and

Downloaded from http://pubs.geoscienceworld.org/gsa/geology/article-pdf/51/10/957/5951746/g51318.1.pdf
by guest

episodic venting of discrete magma batches at the onset of the Huckleberry Ridge supereruption, Yellowstone: Earth and Planetary Science Letters, v. 451, p. 285–297, https://doi.org/10.1016/j.epsl.2016.07.023.

Newcombe, M.E., Plank, T., Barth, A., Asimow, P.D., and Hauri, E., 2020, Water-in-olivine magma ascent chronometry: Every crystal is a clock: Journal of Volcanology and Geothermal Research, v. 398, https://doi.org/10.1016/j.jvolgeores.2020.106872.

Pabst, S., Wörner, G., Civetta, L., and Tesoro, R., 2008, Magma chamber evolution prior to the Campanian Ignimbrite and Neapolitan Yellow Tuff eruptions (Campi Flegrei, Italy): Bulletin of Volcanology, v. 70, p. 961–976, https://doi.org/10.1007/s00445-007-0180-z.

Ruprecht, P., Bergantz, G.W., and Dufek, J., 2008, Modeling of gas-driven magmatic overturn: Tracking of phenocryst dispersal and gathering during magma mixing: Geochemistry, Geophysics, Geosystems, v. 9, Q07017, https://doi.org/10.1029/2008GC002022.

Shamloo, H.I., and Till, C.B., 2019, Decadal transition from quiescence to supereruption: Petrologic investigation of the Lava Creek Tuff, Yellowstone Caldera, WY: Contributions to Mineralogy and Petrology, v. 174, 32, https://doi.org/10.1007/s00410-019-1570-x.

Shamloo, H.I., Till, C.B., and Hervig, R.L., 2021, Multi-mode magnesium diffusion in sanidine: Applications for geospeedometry in magmatic systems: Geochimica et Cosmochimica Acta, v. 298, p. 55–69, https://doi.org/10.1016/j.gca.2021.01.044; corrigendum available at https://doi.org/10.1016/j.gca.2021.07.013.

Spera, F.J., Yuen, D.A., Greer, J.C., and Sewell, G., 1986, Dynamics of magma withdrawal from stratified magma chambers: Geology, v. 14, p. 723–726, https://doi.org/10.1130/0091-7613(1986)14<723:DOMWFS>2.0.CO;2.

Streck, M.J., and Grunder, A.L., 1995, Crystallization and welding variations in a widespread ignimbrite sheet: The Rattlesnake Tuff, eastern Oregon, USA: Bulletin of Volcanology, v. 57, p. 151–169, https://doi.org/10.1007/BF00265035.

Streck, M.J., and Grunder, A.L., 1997, Compositional gradients and gaps in high-silica rhyolites of the Rattlesnake Tuff, Oregon: Journal of Petrology, v. 38, p. 133–163, https://doi.org/10.1093/petroj/38.1.133.

Streck, M.J., and Grunder, A.L., 2008, Phenocryst-poor rhyolites of bimodal, tholeiitic provinces: The Rattlesnake Tuff and implications for mush extraction models: Bulletin of Volcanology, v. 70, p. 385–401, https://doi.org/10.1007/s00445-007-0144-3.

Swenton, V.M., and Streck, M.J., 2022, Pre-eruptive magma configurations and petrogenetic relationships of the Rattlesnake Tuff, Oregon—Insights from spectacularly banded high-silica rhyolite pumices: Frontiers of Earth Science, v. 10, https://doi.org/10.3389/feart.2022.841279.

Till, C.B., Vazquez, J.A., and Boyce, J.W., 2015, Months between rejuvenation and volcanic eruption at Yellowstone caldera, Wyoming: Geology, v. 43, p. 695–698, https://doi.org/10.1130/G36862.1.

Wolff, J.A., Wörner, G., and Blake, S., 1990, Gradients in physical parameters in zoned felsic magma bodies: Implications for evolution and eruptive withdrawal: Journal of Volcanology and Geothermal Research, v. 43, p. 37–55, https://doi.org/10.1016/0377-0273(90)90043-F.

Wright, H.M.N., Folkes, C.B., Cas, R.A.F., and Cashman, K.V., 2011, Heterogeneous pumice populations in the 2.08-Ma Cerro Galán Ignimbrite: Implications for magma recharge and ascent preceding a large-volume silicic eruption: Bulletin of Volcanology, v. 73, p. 1513–1533, https://doi.org/10.1007/s00445-011-0525-5.

Printed in the USA

Downloaded from http://pubs.geoscienceworld.org/gsa/geology/article-pdf/51/10/957/5951746/g51318.1.pdf
by guest